Time-Resolved FTIR Studies of Sensory Rhodopsin II (NpSRII) from *Natronobacterium pharaonis*: Implications for Proton Transport and Receptor Activation

Michael Hein,* Ansgar A. Wegener,† Martin Engelhard,† and Friedrich Siebert*
*Sektion Biophysik, Institut für Molekulare Medizin und Zellforschung, Albert Ludwigs Universität, 79104 Freiburg; and †Max Planck Institut für Molekulare Physiologie, 44227 Dortmund, Germany

ABSTRACT The photocycle of the photophobic receptor from *Natronobacterium pharaonis*, NpSRII, is studied by static and time-resolved step-scan Fourier transform infrared spectroscopy. Both low-temperature static and time-resolved spectra resolve a K-like intermediate, and the corresponding spectra show little difference within the noise of the time-resolved data. As compared to intermediate K of bacteriorhodopsin, relatively large amide I bands indicate correspondingly larger distortions of the protein backbone. The time-resolved spectra identify an intermediate L-like state with surprisingly small additional molecular alterations. With the formation of intermediate M, the Schiff-base proton is transferred to the counterion Asp-75. This state is characterized by larger amide bands indicating larger distortions of the protein. We can identify a second M state that differs only in small-protein bands. Reisomerization of the chromophore to all-*trans* occurs with the formation of intermediate O. The accelerated decay of intermediate M caused by azide results in another red-shifted intermediate with a protonated Schiff base. The chromophore in this state, however, still has 13-*cis* geometry. Nevertheless, the reisomerization is still as slow as under the conditions without azide. The results are discussed with respect to mechanisms of the observed proton pumping and the possible roles of the intermediates in receptor activation.

INTRODUCTION

Archeabacterial phototaxis is mediated by the two photoreceptors sensory rhodopsin I and II. These two pigments enable bacteria like those of *Halobacterium salinarum* to seek optimal light conditions above 500 nm and to avoid harmful ultraviolet (UV) light as well as prevent photooxidative stress in case of high oxygen concentrations in bright sunlight. This latter property is conferred by the photophobic receptor sensory rhodopsin II (reviewed by Schäfer et al., 1999 and Spudich et al., 2000). Generally, the signal transduction chain is based on the two-component system that is well characterized for the chemotactic signaling cascade in e.g., *Escherichia coli* (Rudolph and Oesterhelt, 1996). After the receptor is activated by light, the signal is transferred to its cognate transducer, which in turn triggers the cytoplasmic components that signal the chain and thereby switches the flagellar motor.

Sensory rhodopsin II, originally identified in *H. salinarum* (HsSRII), has also been isolated from *Natronobacterium pharaonis* (NpSRII; Imamoto et al., 1991; Scharf, Pevec, et al., 1992). Because of its superior chemical stability over HsSRII (Scharf, Pevec, et al., 1992), NpSRII has been widely used in recent physiological and biophysical studies. Its crystal structure has been determined to display a fold that is similar to that of the light-activated proton pump bacteriorhodopsin (Luecke et al., 2001; Royant et al., 2001). Differences are found in the cytoplasmic and extracellular channels. The latter changes are mainly due to the replacement of the Asp-96 that is present in bacteriorhodopsin by Phe-86, which is located at a homologous position in NpSRII.

The light-activated photocycle of NpSRII has been studied in great detail (Hirayama et al., 1992; Chizhov et al., 1998). The general mechanism is quite similar to that of bacteriorhodopsin, including the archetypical spectral states K_{NpSRII}, L_{NpSRII}, M_{NpSRII}, N_{NpSRII}, and O_{NpSRII}. Noteworthy is the observation of two M_{NpSRII} states ($M1_{NpSRII}$ and $M2_{NpSRII}$). $M1_{NpSRII}$ decays to $M2_{NpSRII}$ in $\sim$2 ms. This transition, which represents in respect to the UV-visible (UV-vis) spectral range a truly spectrally silent transition, is probably the switch between the ground state and the signaling state. Recent experiments using electron-spin resonance spectroscopy revealed that helix F in a outwardly directed flaplike motion changes the mobility of residues on the cytoplasmic side during the lifetime of M_{NpSRII} (Wegener et al., 2000), which could be later correlated with the $M1_{NpSRII} \rightarrow M2_{NpSRII}$ transition (H. J. Steinhoff and M. Engelhard, unpublished observation).

Further insight into the molecular events that occur during the photocycle have been obtained by static Fourier transform infrared (FTIR) spectroscopy experiments. It can be shown that the proton from the Schiff base has already been transferred to Asp-75 in the M intermediate, which indicates that this neutralization of the Schiff base takes place during the $L_{NpSRII} \rightarrow M_{NpSRII}$ transition (Scharf, Englehard, and Siebert, 1992; Engelhard et al., 1996). For HsSRII, this reaction was also confirmed by an analysis using the corresponding Asp/Asn mutant (Bergo et al., 2000). The retinal chromophore adopts an all-*trans* configuration in the ground

Submitted August 13, 2002, and accepted for publication October 25, 2002.

Address reprint requests to Friedrich Siebert, Hermann-Herderstr. 9, Freiburg, 79104 Germany. Tel.: +49-761-2035396; Fax: +49-761-2035399; E-mail: frisi@biophysik.uni-freiburg.de.

0006-3495/03/02/1208/10 $2.00

state. A light-dark adaptation cannot occur, because the 13-*cis* isomer of retinal is not bound by the protein (Hirayma et al., 1995). In the K_{NpSRII} state, retinal has isomerized to the 13-*cis* configuration (Kandori et al., 2001). It is not yet known at what time the back-isomerization takes place.

For the ion pumps bacteriorhodopsin and halorhodopsin, static time-resolved FTIR spectroscopy has contributed considerably to the understanding of the pumping mechanism (Maeda, 1995; Hackmann et al., 2001). Because it is sensitive to structural changes of both the chromophore and the protein, it is especially suitable for addressing questions about the isomeric state of the chromophore and protein structural changes during the photocycle of NpSRII. By incorporating isotopic labels at specific sites of the protein backbone of bacteriorhodopsin, we provide evidence that in the FTIR difference spectra, the amide I bands reflect local distortions (Hauser et al., 2002). Previously, using time-resolved step-scan FTIR spectroscopy, we unequivocally identified small-protein structural changes during the spectrally silent transitions of bacteriorhodopsin (Rödig et al., 1999) and *N. pharaonis* halorhodopsin (Hackmann et al., 2001) thereby reflecting such backbone distortions, and we also determined the chromophore geometry in the O state of the latter pigment to all-*trans*.

In the present paper, the complete photocycle is analyzed using step-scan FTIR spectroscopy. The data reveal the molecular nature of the $M1_{NpSRII} \rightarrow M2_{NpSRII}$ transition and the isomeric state of retinal in the O_{NpSRII} intermediate without and in the presence of azide. The latter information provides an explanation for a postulated two-photon process under steady-state illumination (Schmies et al., 2000).

MATERIALS AND METHODS

NpSRII was expressed in *E. coli* and purified as described (Shimono et al., 1997; Hohenfeld et al., 1999). The solubilized photoreceptor was reconstituted into purple membrane lipids in accordance with standard procedures (Wegener et al., 2000). These samples did not contain the transducer.

In all infrared measurements, hydrated film samples of NpSRII reconstituted into purple membrane lipids were used. A suspension containing ~100 μg of protein and 500 nM phosphate buffer, pH 8, was dried onto a BaF_2 window, and the film was rehydrated via the water-vapor phase. For the measurements with azide, the molar ratio of azide to NpSRII was 3.3, and the buffer was adjusted to pH 6.5. For measurements in ^2H_2O, the films were completely dried, and 5 μl of ^2H_2O was deposited via the vapor phase in the sealed sample cuvette. This process was repeated five times, after which the final hydration was adjusted.

The low-temperature (103 K) FTIR measurements were performed as described previously (Hackmann et al., 2001) using light of wavelengths between 450 and 500 nm for irradiation. The methods for obtaining time-resolved step-scan infrared spectra were essentially as used before (Rödig et al., 1999; Hackmann et al., 2001). For the largest part of our studies, we used our slower detection system (effective rise time, ~600 ns). Because the photocycle is slow even at 37°C, the repetition rate for signal averaging was 0.5 Hz. To avoid overly long measuring times for a single step-scan run, only four signals were averaged at each sampling position of the interferogram. To achieve a sufficient signal-to-noise ratio, several measurements (16–20) were averaged, which corresponds to 64–80 averages per sampling position. To obtain information about earlier intermediates, we also performed measurements with our fast-detection system (effective rise time, ~30 ns). Because the noise was very large in the early time range of the corresponding time-resolved spectra, a reliable kinetic analysis could not be performed; instead, the spectra of several time-slices were averaged. For sample excitation, the output of an optical parametric oscillator (OPO; Lambda Physik, Göttingen) pumped by the tripled output of a Nd:YAG laser (Brilliant, Quantel) was tuned to 490 nm. Pulse duration was 4 ns. Using neutral-density filters, the pulse energy was reduced to ~1.5 mJ at the sample position. Spectral resolution for the static FTIR measurements was 4 cm^{-1} and for the step-scan measurements was 8 cm^{-1}.

The time-resolved spectra obtained with the slower instrumentation were fitted to a sum of exponentials as described earlier (Rödig et al., 1999; Hackmann et al., 2001). To avoid distortions from the detection rise time, the fit was started 1 μs after the laser flash. The amplitude spectra were further evaluated using the unidirectional reaction scheme without back-reaction as described recently (Rödig et al., 1999; Hackmann et al., 2001). This scheme, which describes transitions between possible fast equilibria of pure states, was used here only as a suitable and direct means of describing the molecular events. For a consistent description, it was necessary to order the reaction sequence according to the increasing time constants derived from the global fit.

RESULTS

General description of the intermediate spectra

Because the cycling time of the NpSRII photoreaction was quite slow, measurements were performed at 37°C, which allowed for a repetition rate of 0.5 Hz for signal averaging during the step-scan measurements. In addition, the transient concentration of O_{NpSRII} increased, which probably played an important role in determining the duration of the photocycle (Chizhov et al., 1998). Although the repetition rate could be enhanced, it was still quite low as compared to that used in our step-scan FTIR measurements of bacteriorhodopsin (Rödig et al., 1999) or halorhodopsin (Hackmann et al., 2001), which made the measurements more difficult and caused a poorer signal-to-noise ratio. This must be taken into account in the analysis of the step-scan data.

Fig. 1 *A* shows the intermediate spectra correlated to the four half-times derived from the global fit, i.e., 7 μs and 1.2, 19, and 101 ms (for evaluation of the data, see Materials and Methods). The corresponding amplitude spectra are shown in Fig. 1 *B*. According to recent time-resolved UV-vis experiments (Chizhov et al., 1998), the photocycle at 37°C is characterized by half-times of 150 ns (extrapolated), 4.5 and 13 μs, and 1, 33, 80, 150, and 350 ms, and we used these data as a reference. The smaller number of exponentials obtained from the time-resolved infrared spectra is due to the larger noise in the infrared data. Comparing the two data sets, it is likely that the 7-μs (FTIR) half-time represents an average of the transitions with half-times of 4.5 and 13 μs that were observed in the UV-vis range, with the larger noise smearing out the two time constants.

The first intermediate identified with the time resolution of 700 ns has to be assigned to the L_{NpSRII} state (Fig. 1 *A*(*a*)). The next intermediate that appeared with a half-time of 7 μs consisted, according to the UV-vis data, of a mixture of mainly M_{NpSRII} and a small amount of L_{NpSRII}, the latter

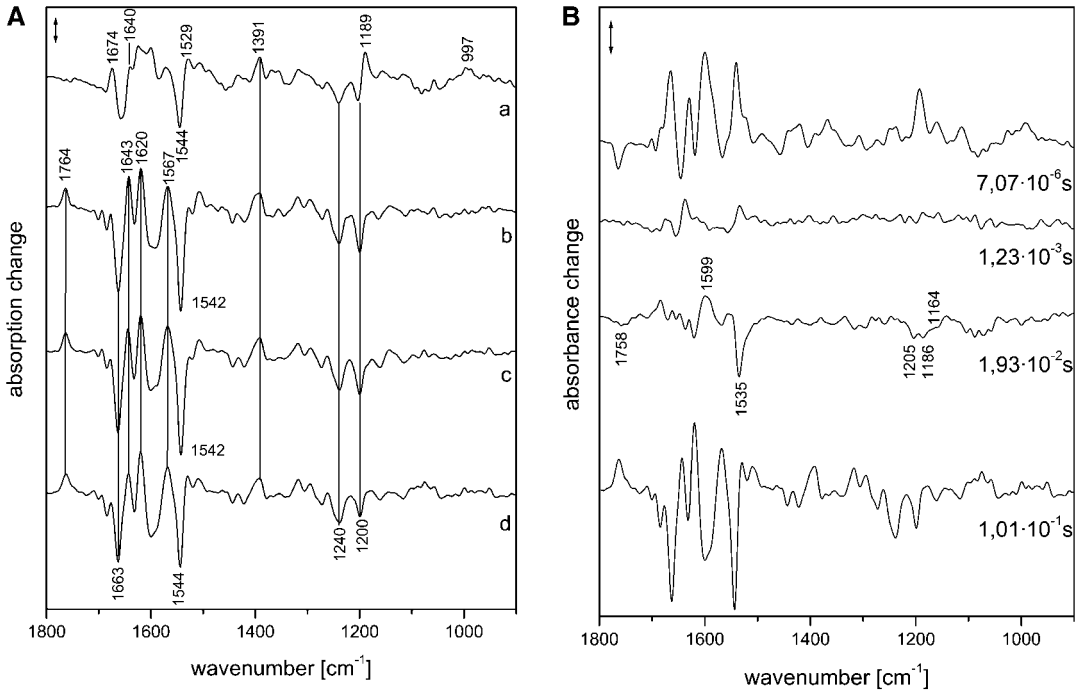

FIGURE 1 (*A*) Intermediate spectra of NpSRII obtained at 37°C with H_2O. Spectra are labeled with the decay half-times of the intermediates: (*a*) 7.07 μs; (*b*) 1.23 ms; (*c*) 19.3 ms; (*d*) 101 ms. Spectral resolution, 8 cm^{-1}. (*B*) Amplitude spectra of NpSRII obtained at 37°C with H_2O from the time-resolved infrared spectra by global fitting to a sum of exponentials. The spectra are labeled with the respective half-times of the exponentials. Spectral resolution, 8 cm^{-1}. Method used to derive the intermediate spectra (*A*) from the amplitude spectra (*B*) is described in Materials and Methods.

decreasing with higher temperature. Only the next intermediate, which appeared with 13 μs, represents a pure M_{NpSRII} state. However, at 37°C, the amount of L_{NpSRII} was very small, and it is plausible that we were unable to detect the transition with a half-time of 13 μs. Thus, we conclude that the second spectrum (Fig. 1 *A* (*b*)) already represented a pure M_{NpSRII} state. Its signatures are the positive band at 1764 cm^{-1} and the lack of a positive band at 1189 cm^{-1}. The former band represents the protonation of the counterion Asp-75 with the deprotonation of the Schiff base (Scharf, Englehard, and Siebert, 1992; Engelhard et al., 1996), whereas the latter indicates the deprotonation of the Schiff base, which caused a drastic reduction of the intensity of the fingerprint bands of the chromophore (Siebert and Mäntele, 1980).

The next transition, with a half-time of 1.2 ms, was also observed in the UV-vis data (1 ms). Its infrared spectrum (Fig. 1 *A* (*c*)) was very similar to that of the previous one. However, subtle differences became evident in the corresponding amplitude spectrum (Fig. 1 *B*, labeled 1.2 ms), which essentially describes the spectral changes between the two intermediates. Only bands in the amide I/II spectral range showed up, which indicates that the protein underwent small distortions of the backbone, but that the chromophore binding pocket was not altered. This observation is in agreement with the UV-vis data, from which a spectrally silent transition was deduced. Obviously, the characterization of this transition as spectrally silent holds true only for the UV-vis spectral range.

Beyond 1 ms, the comparison of the decay times of the infrared vs. the UV-vis measurements reveals larger deviations. Nevertheless, the half-time of 19 ms probably corresponds to that of 30 ms, which characterizes the transition to a mixture of M_{NpSRII} and O_{NpSRII}. From the infrared spectrum of this intermediate (Fig. 1 *A* (*d*)), the contribution of O_{NpSRII} is not directly obvious, although the high temperature should have increased its yield. We also provide evidence that the infrared data indicate a contribution of O_{NpSRII} (see M intermediates), although it is smaller than expected based on the UV-vis measurements. In our data, the half-time of 100 ms describes the transition back to the initial state. However, the half-time of 80 ms observed in the UV-vis experiments describes a transition from the M_{NpSRII}/O_{NpSRII} mixture to an M_{NpSRII}/N_{NpSRII}/O_{NpSRII} equilibrium. Therefore, the process with the half-time of 150 ms, which describes to a large extent the back-reaction to the initial state, better agrees with the last transition that we observed. On the other hand, the last process observed in the UV-vis measurements has no correspondence in the infrared data. Because the amplitude was rather small, this might be due to the larger noise in the infrared data. Later (see Discussion), we discuss possible causes for the deviations in the photocycles if measured using infrared or UV-vis.

The intermediate and amplitude spectra of samples in the presence of ^2H_2O are shown in Fig. 2, *A* and *B*, respectively. Although the half-times partly differ from the values obtained for samples hydrated with H_2O, the spectra

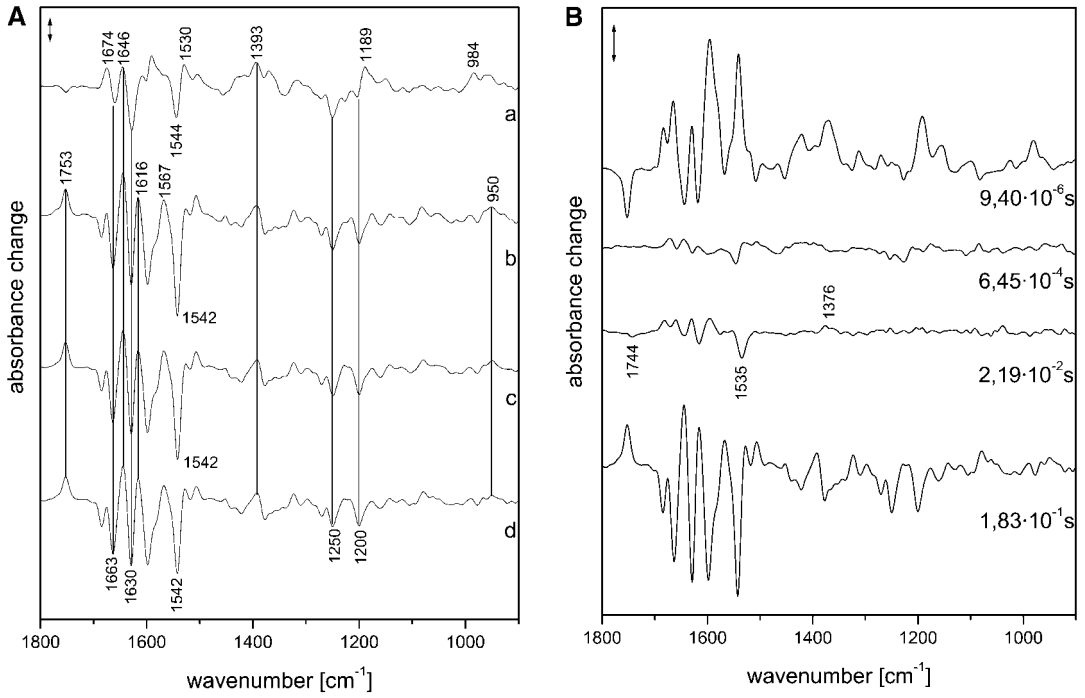

FIGURE 2 (*A*) Intermediate spectra of NpSRII obtained at 37°C with ^2H_2O. Spectra are labeled with the decay half-times of the intermediates: (*a*) 9.4 μs; (*b*) 0.645 ms; (*c*) 21.9 ms; (*d*) 183 ms. Spectral resolution, 8 cm^{-1}. (*B*) Amplitude spectra of NpSRII obtained at 37°C with ^2H_2O from the time-resolved infrared spectra by global fitting to a sum of exponentials. The spectra are labeled with the respective half-times of the exponentials. Spectral resolution, 8 cm^{-1}. Method used to derive the intermediate spectra (*A*) from the amplitude spectra (*B*) is described in Materials and Methods.

demonstrate that they describe the same transitions (see below).

Description of the intermediates

K_{NpSRII} and L_{NpSRII} states

We also measured the photocycle with our faster detection system, which enabled a time resolution of 30 ns (Rödig et al., 1999). However, because of the large size of noise in the data, we were unable to reliably deduce half-times <1 μs. To still be able to deduce an approximate spectrum of K_{NpSRII}, we averaged the spectra that were obtained with high time resolutions over the range from 30 to 100 ns for measurements in H_2O (Fig. 3 (*b*)) and ^2H_2O (Fig. 3 (*c*)). These averaged spectra are very similar to the first intermediate spectra that we identified (Figs. 1 *A* (*a*) and 2 *A* (*a*)). The main differences are the shift of the positive band at 1527 cm^{-1} in the L_{NpSRII} spectra to 1530 cm^{-1} in the spectra of K_{NpSRII} and the larger size of the bands at 1674 and 1640 cm^{-1} in L_{NpSRII}, which both probably represent alterations of amide I bands, because they are little influenced by H/^{2}H exchange. Because ^2H_2O shifts the C═N stretch of the protonated Schiff base of the initial state from 1657 to 1633 cm^{-1}, the remaining bands between 1680 and 1640 cm^{-1} in the ^2H_2O spectrum can be assigned to amide I spectral changes. These bands are considerably more pronounced

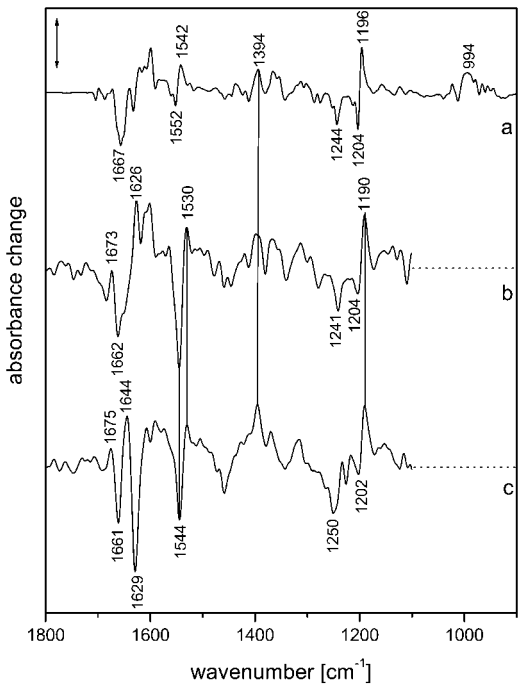

FIGURE 3 Comparison of (*a*) the low-temperature K_{NpSRII} spectrum obtained at 103 K with H_2O, and the time-resolved K_{NpSRII} spectra obtained at 37°C, averaged over 30–100 ns with (*b*) H_2O or (*c*) ^2H_2O. Spectral resolution, 4 cm^{-1} (*a*) or 8 cm^{-1} (*b*) and (*c*). Owing to the large noise below 1100 cm^{-1}, this spectral range was omitted in (*b*) and (*c*).

than those in intermediate K of bacteriorhodopsin, which indicates larger changes of the protein backbone.

The low-temperature K_{NpSRII} spectrum obtained at 103 K (Fig. 3 (*a*)) and the time-resolved K_{NpSRII} spectrum are, within the signal-to-noise ratio of the latter, very similar. In the low-temperature spectrum, the small size of the ethylenic difference band 1552 (−)/1542 (+) as compared to the fingerprint bands between 1270 and 1150 cm^{-1} shows that the ethylenic bands largely overlap and thus the absorption maximum is only slightly red-shifted (Ottolenghi, 1980). This is in agreement with the time-resolved UV-vis data, from which a red-shift of only 11 nm has been deduced (Chizhov et al., 1998), resulting in a shift of the ethylenic mode of only 3 cm^{-1} (see Ottolenghi, 1980 for a correlation of the ethylenic frequencies and absorption maxima). Therefore, the separation of the peaks of the difference band is essentially determined by the half-width of the two ethylenic bands. In contrast to this observation, the time-resolved spectrum exhibits a large negative band at 1544 cm^{-1} and a small positive band at 1530 cm^{-1}. We concluded that the large negative band cannot be assigned to the ethylenic mode of the dark state. Resonance Raman experiments locate this mode at 1548 cm $^{-1}$ (Gellini et al., 2000), which is in agreement with the absorption maximum at 500 nm. Probably an amide II band superimposes at a slightly lower position. This would also reduce the size of the positive ethylenic mode and shift it to lower frequencies, as observed. A further difference between the two spectra (Fig. 3, *a* and *b*) can be seen in the amide I region: the band at 1626 cm^{-1} has considerably lower intensity in the low-temperature spectrum. Thus, both differences are indications for larger distortions of the protein backbone in the time-resolved K_{NpSRII} state which were taken at 37°C. In both K_{NpSRII} states, the amide I bands at 1674 and 1640 cm^{-1} are smaller than those in L_{NpSRII}, which demonstrates that during the $K_{NpSRII} \rightarrow L_{NpSRII}$ transition, the protein undergoes additional structural changes. The positive band at 1527 cm^{-1} in L_{NpSRII} cannot be assigned to the ethylenic stretch, because the absorption maximum is at 500 nm. Therefore, we assign it to protein changes (e.g., amide II or tyrosine). It appears plausible that in K_{NpSRII} the band at 1530 cm^{-1} results from a superposition of the ethylenic stretch and this protein band. It should be noted that a low-temperature K_{NpSRII} spectrum that agrees well with the spectrum shown here has been published before (Kandori et al., 2001). In agreement with those studies, we were unable to stabilize L_{NpSRII} at low temperature.

Surprisingly, in the spectrum of the low-temperature K state, the main hydrogen out-of-plane (HOOP) mode at 997 cm^{-1} is not altered in the L state (although the larger noise in the time-resolved K_{NpSRII} spectrum impedes a reliable identification of this mode, it can be tentatively assigned to a band at the same position; data not shown). This is in contrast to the corresponding K intermediates in bacteriorhodopsin (Weidlich and Siebert, 1993), where the modes of the low-temperature state differ considerably from those of time-resolved KL and L states, and it has been concluded that the chromophore geometries differ considerably. In the latter two states, the twist is confined to the Schiff-base region (Rödig et al., 1999). Because the band in the L_{NpSRII} intermediate is shifted down to 984 cm^{-1} by Schiff-base deuteration (Fig. 2 *A* (*a*)), we assigned it to the 15-HOOP mode. Thus it can be concluded that as in the L state of bacteriorhodopsin, the chromophore in L_{NpSRII} is twisted around the C_{14}–C_{15} single bond.

It was found recently that the HOOP modes of the low-temperature K state of bacteriorhodopsin could also be induced in K_{NpSRII} if the amino acids of the retinal binding pocket were changed to those of bacteriorhodopsin (Shimono et al., 2002). This shows that it is mainly the reduced steric hindrance that allows the chromophore to adopt a more relaxed conformation in the K_{NpSRII} intermediate of wild-type NpSRII.

Measurements after $H/^2H$ exchange often allow an assignment of the C═N stretching mode of the protonated Schiff base, which is shifted down by deuteration. In the spectrum of the L_{NpSRII} intermediate (Fig. 1 *A*), a negative band at 1657 cm^{-1} lost intensity upon deuteration, and instead, a negative band at 1630 cm^{-1} gained intensity (Fig. 2 *A*). Thus we assigned these bands to the C═N stretch of the protonated and deuterated Schiff base of the initial state. In the later intermediates, this shift could still be discerned, although the band at 1657 cm^{-1} was superimposed by another negative band that resulted in a negative band at 1663 cm^{-1} and a positive band at 1643 cm^{-1}. These additional bands were assigned to amide I changes because they were also observed in the presence of ^2H_2O (Fig. 2 *A*). In low-temperature spectra of the K_{NpSRII} intermediate, the band of the deuterated Schiff base was found at 1633 cm^{-1} (data not shown, and see Kandori et al., 2001) within the spectral resolution, which is in agreement with the time-resolved data and also approximately in agreement with resonance Raman spectra (Gellini et al., 2000). However, it was more difficult to assign the corresponding modes to bands of L_{NpSRII}. $H/^2H$ exchange caused pronounced alterations of the positive bands between 1623 and 1600 cm^{-1}, and it was tempting to assign this positive feature to the C═N stretch of L_{NpSRII}. However, these $H/^2H$-induced changes persisted in the M_{NpSRII} intermediate (the first amplitude spectrum was little influenced by $H/^2H$ exchange (Fig. 1 *B* vs. Fig. 2 *B*)), and the positive bands were already present in K_{NpSRII} (H_2O). Thus the C═N stretch of L_{NpSRII} cannot be assigned, and its intensity must be very low.

M intermediates

In the transition from L_{NpSRII} to M_{NpSRII}, besides the characteristic features of the M_{NpSRII} state discussed already, additional molecular changes took place. A band at 1643 cm^{-1} gained intensity overcompensating the negative band

at 1657 cm^{-1} (C=N stretch), and the L_{NpSRII} band at 1674 cm^{-1} lost intensity. Probably these bands represented alterations of amide I modes and indicated distortions of the protein backbone. The L_{NpSRII} band at 1600 cm^{-1} disappeared, and instead, a broad negative band appeared. This is the largest spectral feature of the $L_{NpSRII} \rightarrow M_{NpSRII}$ transition. In this spectral range, the antisymmetric CO_2^- stretch of deprotonated carboxyl groups contributes. Because Asp-75 becomes protonated in the M intermediate, the sign of the spectral changes would be in agreement with such a process. However, the observed spectral changes appear to be far too large to represent only this single protonation step. The largest part, i.e., the positive band at 1600 cm^{-1} in L_{NpSRII} disappearing in M_{NpSRII}, must be caused by additional, yet-unidentified molecular changes. On the other hand, the spectral change around 1360 cm^{-1} that is especially evident in the first amplitude spectrum as a positive band (Fig. 1 *B*) could be caused by the symmetric CO_2^- stretch of deprotonated Asp-75 disappearing in the transition to M_{NpSRII}. This is corroborated by the measurements in ^2H_2O (Fig. 2 *B*). Further changes were observed at 1567 cm^{-1} (positive), which probably represent larger amide II spectral changes in M_{NpSRII}. However, the ethylenic mode of the deprotonated Schiff base chromophore could also contribute. On the other hand, the band at 1527 cm^{-1} of L_{NpSRII}, tentatively assigned to amide II spectral changes, had reduced intensity in M_{NpSRII}. A further large change in the $L_{NpSRII} \rightarrow M_{NpSRII}$ transition involved the ethylenic mode: in the M_{NpSRII} spectrum, the negative band at 1542 cm^{-1} gained intensity. This indicates that a band absorbing in this region disappeared and confirms our earlier conclusion that the ethylenic modes of the initial state and L_{NpSRII} exhibited considerable overlap. (With the formation of the M intermediate, i.e., deprotonation of the Schiff base, there is a large upshift and intensity loss of the ethylenic mode that relieves the overlap between the ground and photoproduct states.) All the spectral features of the $L_{NpSRII} \rightarrow M_{NpSRII}$ transition were especially evident in the amplitude spectrum, where the positive bands represented the L_{NpSRII} state and the negative ones the M_{NpSRII} state. It is noteworthy that this amplitude spectrum was little influenced by $H/^2H$ exchange (Fig. 1 *B* vs. Fig. 2 *B*). This shows that the involved modes coupled only little, if at all, to exchangeable hydrogens.

As already discussed in the general description of the spectra, the transition to the next intermediate involved only small-protein structural changes. Thus this state also had all the characteristics of an M state. The earlier state is called $M1_{NpSRII}$; this later one is termed $M2_{NpSRII}$. Unfortunately, it is presently impossible to interpret these spectral changes in precise molecular terms. Because amide bands show up, we can conclude that the protein backbone undergoes small distortions.

In the subsequent transition, larger spectral changes occurred. We now provide evidence that the O_{NpSRII} state was formed. O_{NpSRII} has an absorption maximum at 535 nm (Chizhov et al., 1998), and thus an ethylenic mode of the chromophore around 1534 cm^{-1} is expected (Ottolenghi, 1980). Indeed, in the corresponding intermediate spectrum, the increase in absorbance at 1529 cm^{-1} could be caused by such a band. But better evidence was obtained from the amplitude spectrum, where the negative band at 1535 cm^{-1} was clearly visible (formation of O_{NpSRII}). The comparison of the last two intermediate spectra shows that the contribution of O_{NpSRII} was small. Therefore, the involved spectral features are better discussed with regard to the amplitude spectrum. Further large changes could be seen around 1597 cm^{-1} and in the amide I spectral range. A peculiar band of the O_{NpSRII} state rose around 1757 cm^{-1} (broad negative band). In the presence of ^2H_2O, this band was shifted to 1744 cm^{-1} (Fig. 2 *B*), which is typical for the C=O stretch of a protonated carboxyl group. Because in both amplitude spectra no corresponding positive band was observed, we assigned the negative band to the protonation of a carboxyl group. Especially, a shift of the band caused by Asp-75 to lower frequencies can be excluded. Thus the positive band observed at 1597 cm^{-1} in the presence of H_2O and ^2H_2O could represent the disappearance of the corresponding antisymmetric CO_2^- stretching mode of deprotonated carboxyl groups. (Evidence for the disappearance of the corresponding symmetric one is obtained from Fig. 2 *B* (22 ms) at 1376 cm^{-1}. However, because this is not so clearly observed in Fig. 1 *B* (19 ms), the assignment is only tentative.) The lack of a clear positive band around 1567 cm^{-1} demonstrates that the corresponding band that rose with the formation of M_{NpSRII} (Fig. 1 *A* (*b*)) cannot represent the ethylenic stretch of the deprotonated Schiff base, but probably must be ascribed to amide II spectral changes. The isomeric state of the chromophore in O_{NpSRII} can be deduced from the fingerprint modes in this amplitude spectrum. The three negative bands at 1164, (shoulder) 1186, and 1205 cm^{-1} are similar to corresponding bands observed at 1168, 1185, and around 1210 cm^{-1} in the transition from N to O in bacteriorhodopsin (Hessling et al., 1993; Rödig et al., 1999). One has to recall that the amplitude spectrum described here reflects the transition from $M2_{NpSRII}$ to O_{NpSRII}, i.e., from an unprotonated Schiff base to a protonated one. Therefore, the negative fingerprint bands essentially represent those of the protonated Schiff base. Because this pattern of fingerprint bands is characteristic of an all-*trans* chromophore, we can conclude that, like in the O intermediate of bacteriorhodopsin and halorhodopsin (Smith et al., 1983; Hackmann et al., 2001), the chromophore is also in this geometry in O_{NpSRII}. In Fig. 2 *B*, these three bands cannot be seen. This is probably due to the larger noise in this spectral region caused by the strong absorbance of ^2H_2O.

Measurements in the presence of azide

Because azide considerably increases the steady-state electric current, which is interpreted as a steady-state proton

translocation (Schmies et al., 2000), we studied the photoreaction in the presence of azide. It has been reported that azide accelerates the reprotonation of the Schiff base (Takao et al., 1998), but without shortening of the photocycle (Schmies et al., 2000). It was concluded that the increase of the proton-pumping rate cannot be explained by the acceleration of the slow photocycle. The pH dependence of the azide effect showed that it is the protonated form of azide that is involved in proton translocation.

In performing the measurements, we faced the problem that to obtain unequivocal spectra, the molar amount of azide should be larger than the molar amount of NpSRII. Owing to the low water content of the infrared samples, this led to an azide concentration exceeding the 1 M level, and according to the time-resolved UV-vis measurements, to a very fast reprotonation of the Schiff base. In addition, the high salt concentration caused a low infrared transmission of the sample and therefore increased the noise in the spectra. It turned out that the spectra showed only small changes in time. The high azide concentration caused such a fast reprotonation of the Schiff base that the M_{NpSRII} intermediate did not accumulate. Together with the larger noise, this made the global fitting procedure of the time-resolved spectra to a sum of exponentials unreliable. To still be able to deduce the main temporal variations, we formed time-averaged spectra whereby the corresponding time ranges were selected from the half-times obtained by the approximate global fit. The last half-time, which described the reformation of the initial state, was reliably determined to 120 ms at 37°C, thereby confirming the observation that azide does not accelerate the photocycle. The results are shown in Fig. 4.

The first spectrum (Fig. 4 (*a*)), which was averaged over the period from 100 to 1040 ns, was very similar to the L_{NpSRII} spectrum shown in Fig. 1 *A* (*a*). The deviations, especially in the amide I spectral range and between 1100 and 1000 cm^{-1}, can be explained by the larger noise. However, the larger intensities of the bands between 1530 and 1500 cm^{-1} represent real spectral differences. Whether they are caused by larger amide II alterations or by a downshifted and increased ethylenic stretching mode is difficult to decide. However, it should be noted that this feature even persisted at later times when Asp-75 became protonated. The fingerprint band characteristic of the 13-*cis* configuration at 1189 cm^{-1} is evident. Although the noise was quite large in the spectral range between 1100 and 1020 cm^{-1} and below 930 cm^{-1}, the HOOP mode at 996 cm^{-1} was by far above the noise level.

The next spectrum, which was averaged between 25 and 61 μs, showed (as expected) the band due to protonation of Asp-75 at 1767 cm^{-1} (Fig. 4 (*b*)). However, in contrast to the M_{NpSRII} spectrum of Fig. 1 *A* (*b*), the positive fingerprint band, although slightly shifted to 1187 cm^{-1}, was still present. This clearly shows that the Schiff base is protonated. This is corroborated by the increase of the band at 1531 cm^{-1}, which was caused by the rise of the corresponding

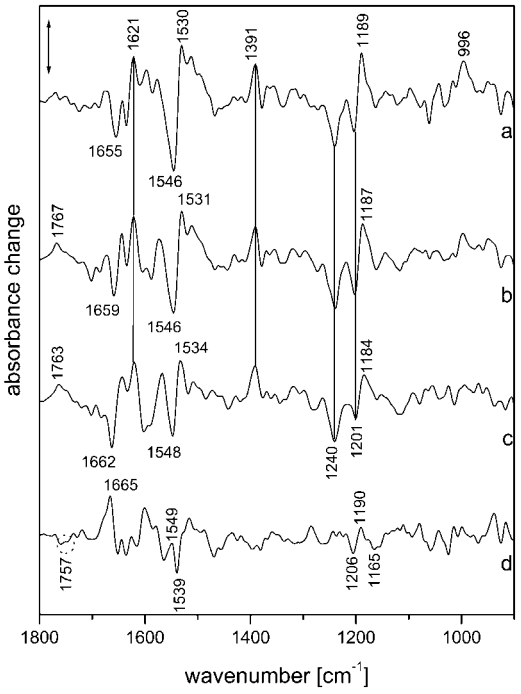

FIGURE 4 Time-resolved difference spectra obtained in the presence of azide at 37°C. Molar ratio of azide to NpSRII was 3.3:1. (*a*) Spectrum averaged between 100 and 1040 ns; (*b*) spectrum averaged between 25 and 61 μs; (*c*) spectrum averaged between 40 and 100 ms; (*d*): weighted difference between (*b*) and (*c*), using the negative band at 1240 cm^{-1} for normalization. Spectral resolution, 8 cm^{-1}.

ethylenic stretching mode. The corresponding absorption maximum must therefore be similar to that of the O_{NpSRII} intermediate, which is in agreement with earlier studies of the influence of azide on the photoreaction (Schmies et al., 2000). The spectra between 1 and 25 μs only show the direct transition from the earlier spectrum (Fig. 4 (*a*)) to this one, without a transient intensity loss of the fingerprint band around 1187 cm^{-1}. Because the time range for protonation of Asp-75 is similar to that observed without azide, we must conclude that immediately after proton transfer from the Schiff base to Asp-75, the Schiff base becomes protonated via protonated azide. Therefore, the species with an unprotonated Schiff base cannot accumulate. The amide I bands indicate that the distortions of the protein backbone are similar to those of M_{NpSRII} (Fig. 1 *A* (*b*)). In contrast to the all-*trans* chromophore geometry in O_{NpSRII}, in this species, the chromophore was still 13-*cis* as indicated by the positive fingerprint band at 1187 cm^{-1}. Therefore, we will call this species MO_{NpSRII}, similar to the NO state identified for mutations of Leu-93 in bacteriorhodopsin (Subramaniam et al., 1991). It is remarkable that the HOOP mode at 996 cm^{-1} was still present in this intermediate, i.e., the chromophore was similarly twisted as in the precursor intermediate and as in L_{NpSRII} in the measurements without azide.

It is tempting to also assign in the first spectrum the larger intensity of the band at 1530 cm^{-1} to the ethylenic mode.

This would indicate that in the presence of azide, the precursor of M_{NpSRII} (or MO_{NpSRII}) has a red-shifted absorption maximum. However, earlier studies on the influence of azide provide no evidence for this, at least up to a 1 M azide concentration. But it appears possible that in our infrared samples, azide was already bound to the cytoplasmatic channel, close to the Schiff base, which would enable its very fast reprotonation. This could cause a red-shift of the absorption maximum of L_{NpSRII} or even bypass its formation.

The analysis of the time-resolved spectra showed that further spectral changes occurred in the 0.1–20-ms time range. Therefore, the last spectrum was averaged over a period from 50 to 100 ms (Fig. 4 (*c*)). The smaller size of the bands is explained by the partial decay to the initial state. The changes with respect to the earlier spectrum can be best estimated by forming the difference between the two spectra using the negative band at 1240 cm^{-1} for normalization. This is shown in Fig. 4 (*d*). It resembles the last amplitude spectrum shown in Fig. 1 *B* (101 ms). The negative bands in the fingerprint region (1205 and 1165 cm^{-1}) show that the chromophore underwent reisomerization to all-*trans*. Here, one must consider that this difference spectrum reflects the transition from MO_{NpSRII} to O_{NpSRII}. Therefore, the strong fingerprint band of MO_{NpSRII} at 1187 cm^{-1} showed up as a positive band around 1190 cm^{-1}. The band at 1757 cm^{-1} indicates that an additional carboxyl group became protonated. Thus, the spectral changes reflect the transition to the O_{NpSRII} intermediate. Interestingly, the ethylenic mode was probably upshifted to 1539 cm^{-1}, indicating that O_{NpSRII} was slightly blue-shifted as compared to MO_{NpSRII}. The larger ethylenic band indicates that considerably more O_{NpSRII} was formed as compared with the measurements without azide (Fig. 1 *A* (*d*)). From our approximate fitting procedure, we obtained a half-time for the MO_{NpSRII} decay of ~25 ms at 37°C. Thus the rate-limiting step of the photocycle was not the back-isomerization of the chromophore (although it was slower than in bacteriorhodopsin), but the relaxation of the protein must control the reformation of the initial state. The last intermediate still contained a large fraction of MO_{NpSRII}, which indicates that the lifetime of protein states that favor the 13-*cis* geometry of the chromophore is rather long.

DISCUSSION

In the analysis of the time-resolved infrared spectra obtained at 37°C, we were able resolve four intermediates: L_{NpSRII}, $M1_{NpSRII}$, $M2_{NpSRII}$, and MO_{NpSRII}. The analysis of the spectra obtained with 30-ns time resolution also provided evidence for the existence of a K_{NpSRII} state that is very similar to the L_{NpSRII} state, with the exception of small alterations in the amide I/II spectral range. Up to several milliseconds, the analysis was in good agreement with earlier time-resolved UV-vis studies (Chizhov et al., 1998). The deviations observed for the later times can probably be explained by the low water content of the infrared samples. Preliminary experiments with steady-state illumination using a diamond-attenuated total-reflection cell or the sandwich-sample technique (Vogel and Siebert, 2001), which both guarantee a natural aqueous environment, showed that as compared with the film samples, considerably more O_{NpSRII} accumulated as expected from the photocycle. Thus, hydration sensitively influenced the photocycle after formation of the M_{NpSRII} intermediates.

The time-resolved UV-vis spectra showed only a small red-shift (11 nm) for K_{NpSRII} (Chizhov et al., 1998). This is in contrast to earlier published low-temperature spectra, which indicated red-shifts of 25 and 35 nm for two K_{NpSRII} species (Hirayama et al., 1992). As discussed, the small size of the ethylenic modes in the low-temperature infrared spectrum presented here is in better agreement with the small red-shift. It is not clear what caused the differences, but the different sample preparations, namely, NpSRII reconstituted into lipids vs. solubilized NpSRII, may have contributed. The time-resolved spectra of K_{NpSRII} of samples hydrated with ^2H_2O where the C═N mode of the Schiff base was shifted to 1630 cm^{-1} clearly reveal amide I bands between 1700 and 1640 cm^{-1} that are considerably larger than those observed for the K intermediate of bacteriorhodopsin. This indicates that in this early intermediate, the protein backbone underwent correspondingly larger distortions. Interestingly, photoacoustic measurements provided evidence for considerable volume changes for K_{NpSRII}, but a much smaller change has been deduced for K of bacteriorhodopsin (Losi et al., 1999).

We have clearly identified a transition ($M1_{NpSRII} \rightarrow M2_{NpSRII}$) that only involves changes of the protein that is in agreement with the UV-vis studies describing a spectrally silent transition (in the UV-vis) with the same half-time. A similar transition has been described for halorhodopsin, and the corresponding protein changes have been invoked as an indication for the accessibility change of the anion from the extracellular to the cytoplasmic side (Hackmann et al., 2001; Chizhov and Engelhard, 2001). The functional role of this transition in NpSRII is not yet clear. It could be that in view of the influence of hydration on the millisecond part of the photocycle, the differences between $M1_{NpSRII}$ and $M2_{NpSRII}$ are actually larger if excess water is present. In view of these data, it is noteworthy that recent electron paramagnetic resonance experiments indicate an outward movement of helix F during the $M1_{NpSRII} \rightarrow M2_{NpSRII}$ transition (M. Engelhard and J. Steinhoff, unpublished results). An unequivocal correlation of the amide-band changes and the helix-F movement may be accomplished by using site-specific isotope labeling of peptide bonds. Using bacteriorhodopsin as a model system, we recently showed by selective incorporation of a ^{13}C label into a single peptide group (carbonyl position) that especially positions in the

middle to extracellular part of helices 3 and 6 contribute to the amide I changes in the N state (Hauser et al., 2002). This has been interpreted by the assumption that at these positions, the movements of these helices cause distortions in the backbone.

The most striking observation is the identification of the 13-*cis* geometry of the chromophore in the MO_{NpSRII} state accumulated in the presence of azide, whereas in the subsequent O_{NpSRII} intermediate the conformation was turned to all-*trans*. This observation could explain the increase in steady-state proton pumping in the presence of azide, which has been explained by a two-photo process (Schmies et al., 2000). Because the Schiff base was already reprotonated, the long-lived MO_{NpSRII} intermediate could easily absorb a second photon. This process probably caused the *cis-trans* back-isomerization of the retinal chromophore and thereby shortened the photocycle. The higher turnover number would result in an increased photostationary current as was actually observed.

At present, we cannot identify the second carboxyl group that became protonated with the formation of O_{NpSRII}. In the case of bacteriorhodopsin, some evidence has been obtained for protonation of Asp-212 with the formation of O. One interpretation has been that the proton is transferred from Asp-85 to Asp-212 (Dioumaev et al., 1999). Such a proton exchange between two carboxyl groups can be excluded, because in the corresponding amplitude spectrum (Fig. 1 *B* (19 ms)) in the spectral range where protonated carboxyl groups show up, we observed only a negative band. A proton circulation involving an additional titratable group has been proposed for Schiff-base reprotonation (Sasaki and Spudich, 1999). However, in this case, a deprotonation would have been expected. The band position at 1758 cm^{-1} indicated that the protonated carboxyl group was not strongly hydrogen-bonded, thereby excluding a group exposed to the aqueous phase. The only internal carboxyl group is Asp-201, the equivalent of Asp-212 in bacteriorhodopsin. If the band were caused by this residue, it would not pick up the proton from Asp-75. The positive charge of the Schiff base and the neutralization of Asp-75 and Asp-201 would probably require a compensation of the positive charge of Arg-72. Thus it could be that there is proton transfer from this residue to Asp-201. Interestingly, the protonation state of Arg-72 has been recently suggested as taking part in controlling the pK_a of the Schiff base in the dark state (Iwamoto et al., 2002). Because Asp-201 is close to the Schiff base, a proton transfer from Arg-72 to Asp-201 appears possible if the corresponding pK_a values were regulated by the protein environment. The trigger for this proton transfer could be conformational changes that relocate either of these residues or both in a less-polar environment. However, it has to be emphasized that this interpretation is speculative. The small size of the band is probably due to the small amount of O formed in this transition. A more thorough analysis of the molecular events involved with the formation of O requires its considerably larger accumulation. This can be achieved, as mentioned above, at a much higher degree of hydration that is obtainable with sandwich samples. Such experiments are in progress.

It is remarkable that the reprotonation of the Schiff base in MO_{NpSRII} does not, as compared to $M2_{NpSRII}$, accelerate the reisomerization, in that the barrier of the 13,14 double bond is reduced. This shows that it is the protein conformation that determines the rate of back-isomerization. Furthermore, because O_{NpSRII} is in equilibrium with considerable amounts of either M_{NpSRII} or MO_{NpSRII}, the back-isomerization is essentially controlled by the long lifetime of the state with M conformation, which is thought to represent the signaling state. This temporal stability may be important to convey the information of light absorption by the receptor to the interacting transducer.

The authors thank M. Schumacher for excellent technical help and T. Savopol for critical reading of the manuscript.

This work was supported by Deutsche Forschungsgemeinschaft Grants AZ EN 87/10-4,5 (to M. Engelhard) and AZ SI 278/18-3,4 (to F. Siebert) and by Fonds der Chemischen Industrie (to F. Siebert).

REFERENCES

Bergo, V., E. N. Spudich, K. L. Scott, J. L. Spudich, and K. J. Rothschild. 2000. FTIR analysis of the SII_{540} intermediate OD sensory rhodopsin II: Asp-73 is the Schiff base proton acceptor. *Biochemistry* 39:2823–2830.

Chizhov, I. and M. Engelhard. 2001. Temperature and halide dependence of the photocycle of halorhodopsin from *Natronobacterium pharaonis*. *Biophys. J.* 81:1600–1612.

Chizhov, I. V., G. Schmies, R. Seidel, J. R. Sydor, B. Lüttenberg, and M. Engelhard. 1998. The photophobic receptor from *Natronobacterium pharaonis*: temperature and pH dependence of the photocycle of sensory rhodopsin II. *Biophys. J.* 75:999–1009.

Dioumaev, A. K., L. S. Brown, R. Needleman, and J. K. Lanyi. 1999. Fourier transform infrared spectra of a late intermediate of the bacteriorhodopsin photocycle suggest transient protonation of Asp-212. *Biochemistry* 38:10070–10078.

Engelhard, M., B. Scharf, and F. Siebert. 1996. Protonation changes during the photocycle of sensory rhodopsin II from *Natronobacterium pharaonis*. *FEBS Lett.* 395:195–198.

Gellini, C., B. Luttenberg, J. Sydor, M. Engelhard, and P. Hildebrandt. 2000. Resonance Raman spectroscopy of sensory rhodopsin II from *Natronobacterium pharaonis*. *FEBS Lett.* 472:263–266.

Hackmann, C., J. Guijarro, I. Chizhov, M. Engelhard, C. Rödig, and F. Siebert. 2001. Static and time-resolved step-scan FTIR investigations of the photoreaction of halorhodopsin from *Natronobacterium pharaonis*: consequences for the anion translocation mechanism. *Biophys. J.* 81: 394–406.

Hauser, K., M. Engelhard, N. Friedman, M. Sheves, and F. Siebert. 2002. Interpretation of amide I difference bands observed during protein reactions using site-directed isotopically labeled bacteriorhodopsin as a model system. *J. Phys. Chem. A* 106:3553–3559.

Hessling, B., G. Souvignier, and K. Gerwert. 1993. A model-independent approach to assigning bacteriorhodopsin's intramolecular reactions to photocycle intermediates. *Biophys. J.* 65:1929–1941.

Hirayama, J., Y. Imamoto, Y. Shichida, N. Kamo, H. Tomioka, and T. Yoshizawa. 1992. Photocycle of phoborhodopsin from haloalkaliphilic

bacterium (*Natronobacterium pharaonis*) studied by low-temperature spectrophotometry. *Biochemistry* 31:2093–2098.

Hirayma, J., N. Kamo, Y. Imamoto, Y. Shichida, and T. Yoshizawa. 1995. Reason for the lack of light-dark adaptation in *pharaonis* phoborhodopsin: reconstitution with 13-*cis*-retinal. *FEBS Lett*. 364:168–170.

Hohenfeld, I. P., A. A. Wegener, and M. Engelhard. 1999. Purification of histidine tagged bacteriorhodopsin, *pharaonis* halorhodopsin, and *pharaonis* sensory rhodopsin II functionally expressed in *Escherichia coli*. *FEBS Lett*. 442:198–202.

Imamoto, Y., Y. Shichida, T. Yoshizawa, H. Tomioka, T. Takahashi, K. Fujikawa, N. Kamo, and Y. Kobatake. 1991. Photoreaction cycle of phoborhodopsin studied by low-temperature dpectrophotometry. *Biochemistry* 30:7416–7424.

Iwamoto, M., Y. Furutani, Y. Sudo, K. Shimono, H. Kandori, and N. Kamo. 2002. Role of Asp193 in chromophore-protein interaction of *pharaonis* phoborhodopsin (sensory rhodopsin II). *Biophys. J*. 83:1130–1135.

Kandori, H., K. Shimono, Y. Sudo, M. Iwamoto, Y. Shichida, and N. Kamo. 2001. Structural changes of *pharaonis* phoborhodopsin upon photoisomerization of the retinal chromophore: infrared spectral comparison with bacteriorhodopsin. *Biochemistry* 40:9238–9246.

Losi, A., A. A. Wegener, M. Engelhard, W. Gärtner, and S. E. Braslavsky. 1999. Time-resolved absorption and photothermal measurements with recombinant sensory rhodopsin II from *Natronobacterium pharaonis*. *Biophys. J*. 77:3277–3286.

Luecke, H., B. Schobert, J. K. Lanyi, E. N. Spudich, and J. L. Spudich. 2001. Crystal structure of sensory rhodopsin II at 2.4 Å resolution: insights into color tuning and transducer interaction. *Science* 293:1499–1503.

Maeda, A. 1995. Application of FTIR spectroscopy to the structural study on the function of bacteriorhodopsin. *Isr. J. Chem*. 35:387–400.

Ottolenghi, M. 1980. The photochemistry of rhodopsin. *In* Advances in Photochemistry, Vol. 12. J. N. Pitts, G. S. Hammond, K. Gollnik, and D. Grosjean, editors. Wiley-Interscience, New York. 97–200.

Rödig, C., I. V. Chizhov, O. Weidlich, and F. Siebert. 1999. Time-resolved step-scan FTIR spectroscopy reveals differences between early and late M intermediates of bacteriorhodopsin. *Biophys. J*. 76:2687–2701.

Royant, A., P. Nollert, K. Edman, R. Neutze, E. M. Landau, E. Pebay-Peyroula, and J. Navarro. 2001. X-ray structure of sensory rhodopsin II at 2.1-Å resolution. *Proc. Natl. Acad. Sci. USA* 98:10131–10136.

Rudolph, J. and D. Oesterhelt. 1996. Deletion analysis of the operon in the archeon *Halobacterium salinarium*. *J. Mol. Biol*. 258:548–554.

Sasaki, J. and J. L. Spudich. 1999. Proton circulation during the photocycle of sensory rhodopsin II. *Biophys. J*. 77:2145–2152.

Schäfer, G., M. Engelhard, and V. Müller. 1999. Bioenergetics of the archaea. *Microbiol. Mol. Biol. Rev*. 63:570–620.

Scharf, B., M. Engelhard, and F. Siebert. 1992. A carboxyl group is protonated during the photocycle of the photophobic receptor psR-II from Natronobacterium pharaonis. *In* Structure and Function of Retinal Proteins, Vol. 221. J.-L. Rigaud, editor. Colloque INSERM/John Libbey Eurotext Ltd. 317–320.

Scharf, B., B. Pevec, B. Hess, and M. Engelhard. 1992. Biochemical and photochemical properties of the photobic receptors from Halobacterium halobium and Natronobacterium pharaonis. *Eur. J. Biochem*. 206:359–366.

Schmies, G., B. Lüttenberg, I. V. Chizhov, M. Engelhard, A. Becker, and E. Bamberg.2000. Sensory rhodopsin II from the haloalkaliphilic *Natronobacterium pharaonis:* light-activated proton transfer reactions. *Biophys. J*. 78:967–976.

Shimono, K., Y. Furutani, H. Kandori, and N. Kamo. 2002. A *pharaonis* phoborhodopsin mutant with the same retinal binding site residues as in bacteriorhodopsin. *Biochemistry* 41:6504–6509.

Shimono, K., M. Iwamoto, M. Sumi, and N. Kamo. 1997. Functional expression of *pharaonis* phoborhodopsin in *Escherichia coli*. *FEBS Lett*. 420:54–56.

Siebert, F. and W. Mäntele. 1980. Investigation of the rhodopsin/meta I and rhodopsin/meta II transitions of bovine rod outer segments by means of kinetic infrared spectroscopy. *Biophys. Struct. Mech*. 6:147–164.

Smith, S. O., J. A. Pardoen, P. P. J. Mulder, B. Curry, J. Lugtenburg, and R. A. Mathies. 1983. Chromophore structure in bacteriorhodopsin's O_{640} photointermediate. *Biochemistry* 22:6141–6148.

Spudich, J. L., C.-S. Yang, K.-H. Jung, and E. N. Spudich. 2000. Retinylidene proteins: structures and functions from archae to humans. *Annu. Rev. Cell Dev. Biol*. 16:365–392.

Subramaniam, S., D. A. Greenhalgh, P. Rath, K. J. Rothschild, and H. G. Khorana. 1991. Replacement of leucine-93 by alanine or threonine slows down the decay of the N and O intermediates in the photocycle of bacteriorhodopsin: implications for proton uptake and 13-*cis*-retinal—all-*trans*-retinal reisomerization. *Proc. Natl. Acad. Sci. USA* 88:6873–6877.

Takao, K., T. Kikukawa, T. Araiso, and N. Kamo. 1998. Azide accelerates the decay of M-intermediate of *pharaonis* phoborhodopsin. *Biophys. Chem*. 73:145–153.

Vogel, R. and F. Siebert. 2001. Conformations of the active and inactive states of opsin. *J. Biol. Chem*. 276:38487–38493.

Wegener, A. A., I. Chizhov, M. Engelhard, and H. J. Steinhoff. 2000. Time-resolved detection of transient movement of helix F in spin-labelled pharaonis sensory rhodopsin II. *J. Mol. Biol*. 301:881–891.

Weidlich, O. and F. Siebert. 1993. Time-resolved step-scan FT-IR investigations of the transition from KL to L in the bacteriorhodopsin photocycle: identification of chromophore twists by assigning hydrogen-out-of-plane (HOOP) bending vibrations. *Appl. Spectrosc*. 47:1394–1400.